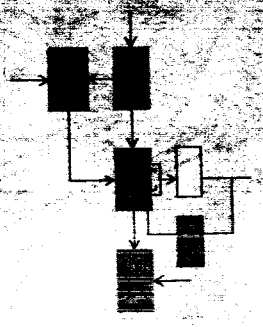

ESL-TM-162
DSR 8836

A VIBRATORY ACOUSTIC GYROSCOPE

Research Grant No. NSG-149-61

by
R. Swerdlow and J. G. Whitman, Jr.

December, 1962

Electronic Systems Laboratory

MASSACHUSETTS INSTITUTE OF TECHNOLOGY, CAMBRIDGE 39, MASSACHUSETTS

Department of Electrical Engineering

December 1962 DSR 8836 Copy 11

Technical Memorandum-ESL-TM-162

A VIBRATORY ACOUSTIC GYROSCOPE

by

Richard Swerdlow

and

John G. Whitman, Jr.

The preparation and publication of this report, including the research on which it is based was sponsored by the National Aeronautics and Space Administration under Research Grant No. NSG-149-61. This report is published for information purposes only and does not represent recommendations or conclusions of the sponsoring agency. Reproduction in whole or part is permitted for any purpose of the United States Government.

Approved by: George C. Newton, Jr.
George C. Newton, Jr.
Associate Director

Electronic Systems Laboratory
Department of Electrical Engineering
Massachusetts Institute of Technology
Cambridge 39, Massachusetts

TABLE OF CONTENTS

COMMENT

The following discussion is issued as a memorandum for reference only. It is intended to be neither a terminal report or an interim report, but rather an indication of some but not all considerations relating to a device which did not seem to offer as much promise as others that were being considered concurrently. To obtain conclusive results a number of problem areas requiring complex theoretical analysis (which would not necessarily be conclusive) or extensive experimental work would have to be investigated. Because of the questionable value of further research, the general area has been temporarily abandoned pending the evaluation of apparently more fruitful schemes.

LIST OF FIGURES

CHAPTER I

INTRODUCTION AND SUMMARY

A. INTRODUCTION

This memorandum summarizes the investigation to date of one type of vibratory output angular motion sensing instrument. The instrument is a member of the class utilizing the Coriolis coupling mechanism. The principles of acoustic resonance in a high Q fluid sensing system are applied to the problem of amplifying a low level coupling pressure signal and sensing it with state of the art pressure transducers. The particular configuration of the instrument that has been chosen for the analysis illustrates the main features of the operation of an angular motion sensor of this type, yet is sufficiently simple to allow detailed analytical calculations; this configuration will be understood not to represent the optimum for particular instrument design. A number of designs which incorporate features of practical importance not significant to the present performance analysis are found in a patent by Granquist.[1*]

Loss mechanisms determining the pressure amplification which can be attained in the fluid resonator are discussed in detail below, and a thermal noise analysis is presented which yields an expression for a thermal noise-equivalent angular rate input. A number of areas in which the need for continued investigation is indicated are pointed out; and, in particular, the limitations of the simple noise analysis are recognized.

Expressions for noise pressure, thermal threshold rate, and sensitivity which are derived are felt to be more significant for their analytical form than for the quantitative figures which they yield upon insertion of selected fluid parameters and apparatus dimensions. Nevertheless, these quantitative results are felt to be approximately correct in indicating the potential worth of this type of angular motion sensor. It is emphasized that a more extensive investigation of a number of areas will be necessary before firm conclusions can be drawn in this regard.

---

* Superscripts refer to numbered items in the Bibliography.

B. PRINCIPLES OF OPERATION

On the apparatus depicted in Fig. 1.1 a fluid of density ρ_d and speed of sound transmission c_d is driven in a half wavelength resonant mode within a tank of rectangular cross section oriented along the y-axis. The envelopes of the pressure and velocity distributions within this driver tank appear in Fig. 1.2a. Located on either side of the driver tank at its center and extending along the x-axis are two quarter wave sensing tanks filled with a second fluid medium characterized by ρ_T and c_T. These tanks are coupled to the driver tank through flexible diaphragms (having no bending stiffness) that transmit pressure variations, and they are terminated at their outer extremities with pressure sensitive transducers. Figure 1.2b depicts the pressure and velocity distribution envelopes within the sensing tanks.

In order to understand the operation of the instrument, imagine an angular rate $\bar{\Omega}$ to be impressed about the z-axis. Each mass element dm having a velocity vector $\dot{\bar{\xi}}$ experiences a Coriolis force given by

$$\overrightarrow{df_c} = 2\,dm\ \dot{\vec{\xi}} \times \vec{\Omega} = 2\rho_d\ \dot{\vec{\xi}} \times \vec{\Omega}\, dV \qquad (1.1)$$

In particular, the velocity vector of the mass elements within the driver tank is along the y-axis, and thus the force on each such element is directed along the x-axis normal to the pressure-sensitive diaphragms at the entrances to the sensor tanks. These diaphragms are therefore subjected to a pressure variation given by

$$p_c = 2\rho_d \int_{-d_{d/2}}^{d_{d/2}} \dot{\vec{\xi}} \times \vec{\Omega} \cdot \overrightarrow{dl} \qquad (1.2)$$

where dl is a path parallel to the x-axis and d_d is the width of the driver tank between the two diaphragms.

Referring to Fig. 1.2a, the particle velocity within the driver tank is

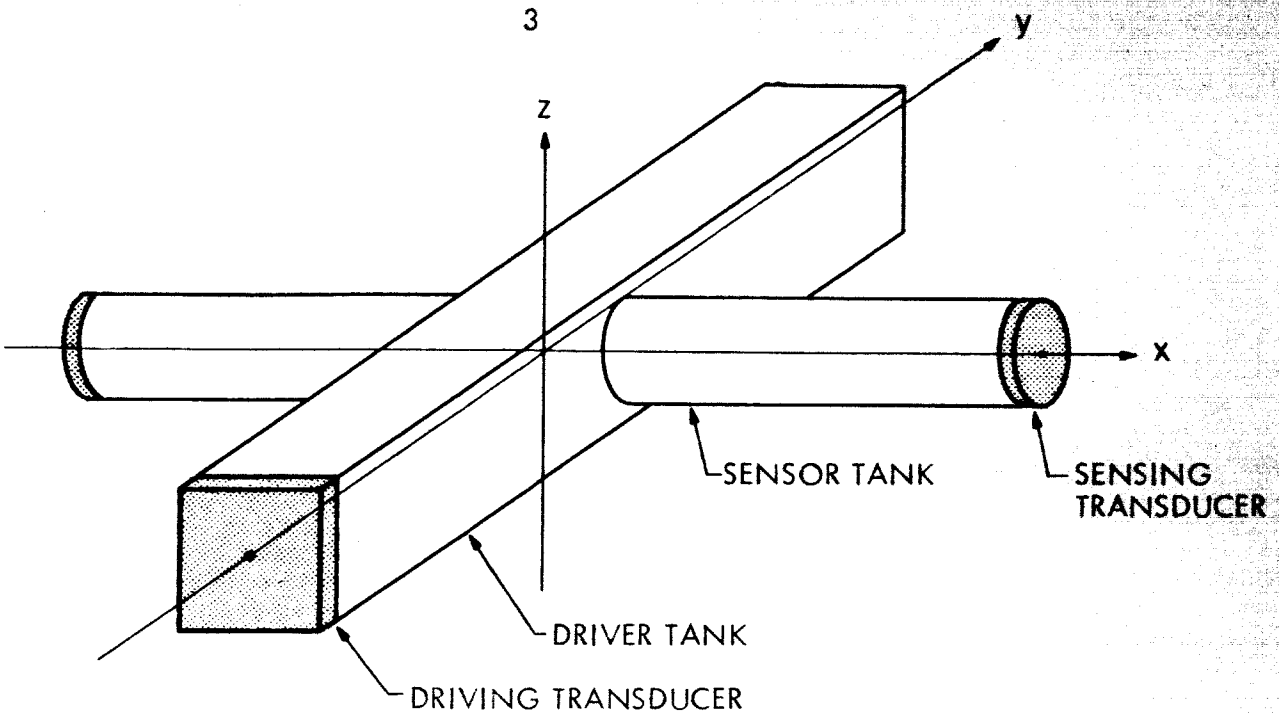

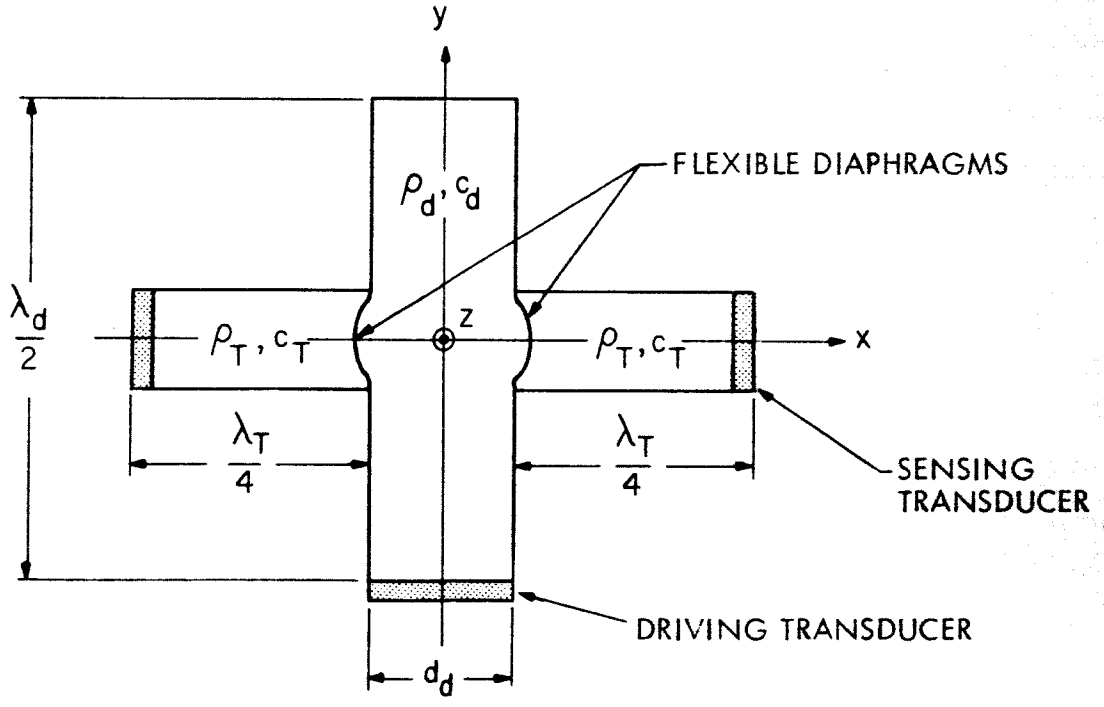

Fig.1-1 Perpective and Top View of Possible Acoustic Angular Motion Sensor

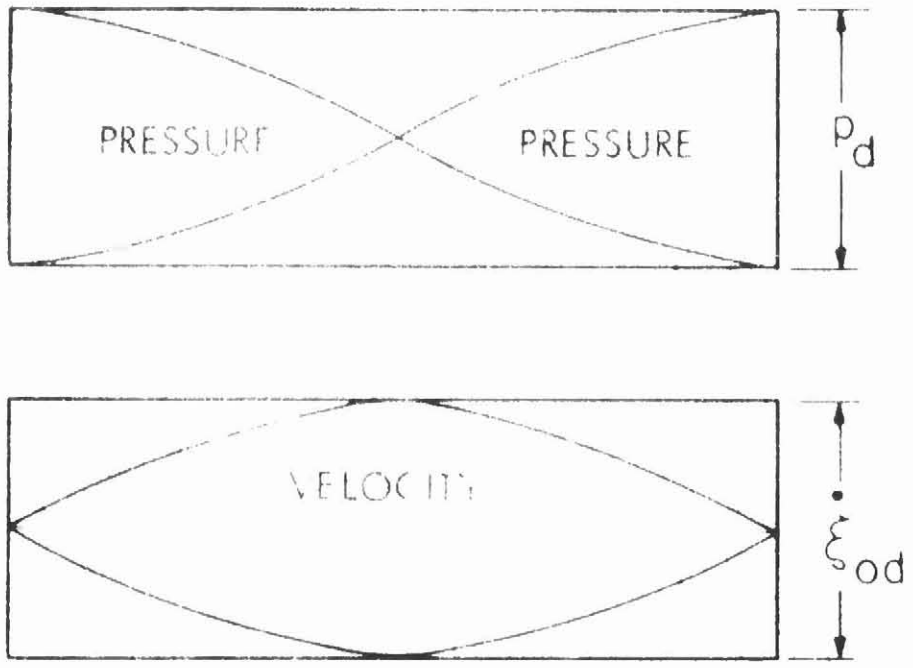

a) Driver Tank

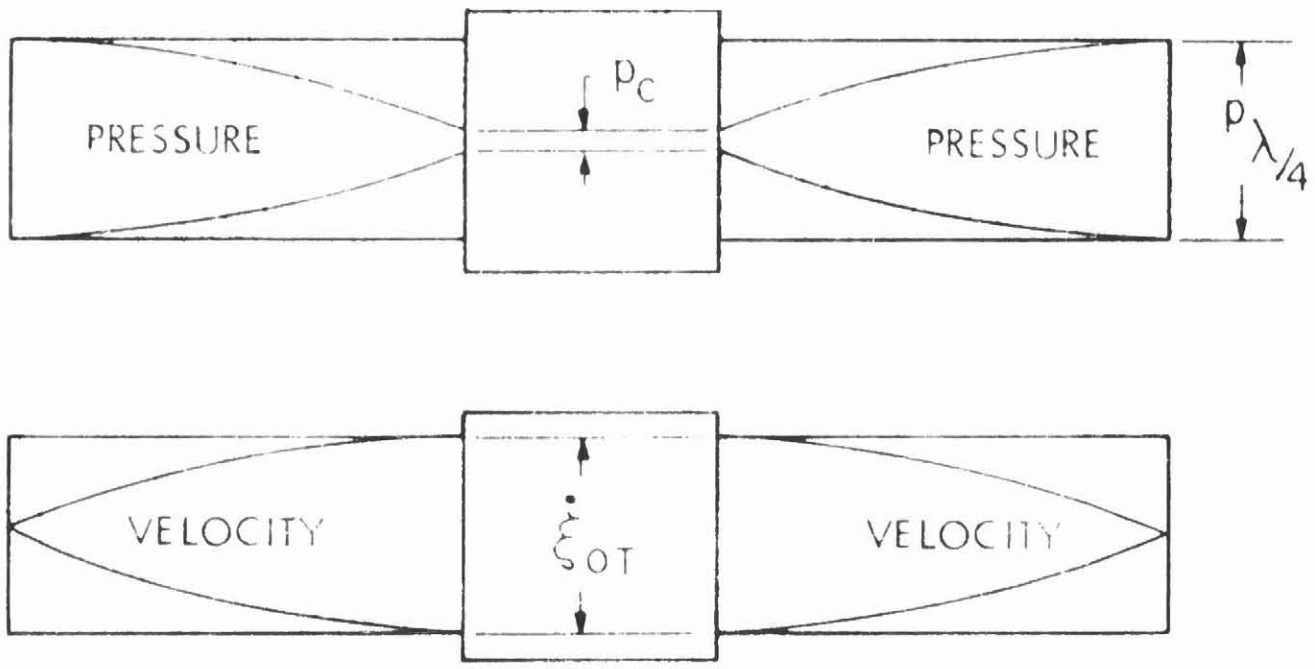

b) Sensor Tanks

Fig.1-2 Pressure and Velocity Distribution within Driver and Sensor Tanks

$$\dot{\vec{\xi}} = \vec{i}_y \dot{\xi}_o (\cos \omega_d t) \cos \frac{2\pi y}{\lambda_d} \tag{1.3}$$

and the applied rate is

$$\vec{\Omega} = \vec{i}_z \Omega(t) \tag{1.4}$$

In calculating the pressure variation at the entrances to the sensor tanks the spatial cosine can be taken as unity since the tank openings occupy only a small region at the center of the driver tank, and thus the magnitude of the pressure on the diaphragms is given by

$$p_c = 2d_d \rho_d \dot{\xi}_o (\cos \omega_d t) \Omega(t)$$

$$= 2d_d \frac{P_d}{c_d} (\cos \omega_d t) \Omega(t) \tag{1.5}$$

Note that in the absence of an applied rate, the sensor tanks ideally remain unexcited. If a rate or rate component about the z-axis is present, however, energy is coupled from the driver into the sensor tanks through the action of the **Coriolis** pressure. The pressure variations coupled into the sensor tanks in this way excite the resonant mode of these tanks as shown in Fig. 1.2b, and the transducers at the pressure antinodes at the outer end of the tanks sense the greatly magnified pressure signal that is proportional to the impressed angular rate.

Equation 1.5 shows p_c to be a suppressed carrier signal; and since the frequencies contained in $\Omega(t)$ will be small with respect to the driving frequency ω_d, p_c will have no frequency components except very near ω_d. This is undesirable since the high level signal of frequency ω_d in the driver tank will certainly couple into the sensor section of the instrument even with no rate applied. Previous investigators of vibratory output angular motion sensors have found the **resulting** large zero rate output signals (and cross-coupling signals in general) to be a major problem.[2, 3] The cross-coupling problem can be avoided in theory by shifting the rate signal in the sensing tanks to frequencies far enough separated from the driver frequency so that linear filtering can be used to recover the former even when appreciable cross coupling exists. The required frequency shift can be produced by a

process of double-modulation in which the entire instrument is given a spin velocity ω_s about the driving axis, in this case the y-axis. This spin moves the angular rate information into side bands at $\omega_d \pm \omega_s$ where it can be recovered using a band-pass filter and demodulator. The filtering can be accomplished at least partially, by constructing the sensing tanks to be resonant at one or the other of the side band frequencies.

The use of a double-modulation scheme has the additional advantage of rendering the instrument sensitive to input rates about the x-axis as well as the z-axis, for it is apparent that the spinning motion of the transducer makes the x and z axes distinguishable from one another only through a 90° phase difference. The x and z rate components are then identified in the composite output signal by phase-sensitive demodulation. An estimate of the degree of decoupling obtainable through double modulation techniques is being experimentally evaluated by the consideration of another type of vibrating gyroscope. Status Report ESL-SR-158 comments on this area of investigation.

All performance calculations in the present memorandum rest upon the hypothesis that some such scheme as double modulation permits the reduction of mechanical cross-coupling to negligible levels.

C. THEORETICAL RESULTS

An investigation of loss mechanisms relevant to a resonant fluid system discloses that the major mechanism of loss is shear in the boundary layer where the fluid meets the walls of its containing vessel. It can be shown that in tanks whose radius is large with respect to boundary layer skin depth the modes of standing waves within the tank are little changed from the lossless case, and by equating the per unit length boundary layer losses to an assumed distributed power loss per unit length it is possible to write the equations of motion for a lossy medium and to show that the losses are equivalent to a viscous damping and a mass loading which lowers the speed of sound in the medium slightly.

The major effect of the losses is to lower the Q which characterizes the resonant system. Q is calculated from its definition as the ratio of the total system stored energy to the energy dissipated per cycle. This calculation shows that Q of the sensing tank is given by Eq. 1.6

$$Q_I = r/\Delta = r\sqrt{\frac{\rho\omega}{2\mu}} \qquad (1.6)$$

where r is the radius of the sensing tank Δ is the skin depth, and μ is the viscosity of the filling fluid.

The amplification factor between the low level Coriolis coupling pressure and the pressure level at the outer end of the sensor tanks is calculated by equating the power coupled into the tanks to that dissipated within the tanks in the steady state. If $P_{\lambda/4}$ represents the pressure at the end of the quarter wave sensor tanks and p_c is the Coriolis pressure coupled in at the diaphragms, the amplification factor is found to be given by Eq. 1.7

$$\frac{P_{\lambda/4}}{p_c} = \frac{4}{\pi} Q_\tau = \frac{4}{\pi}\frac{r}{s} \qquad (1.7)$$

A simple thermal noise analysis assigns an energy of 1/2 KT to both the time average kinetic and potential energy stored within the resonant system, and the root mean square thermal noise pressure is found to be given by Eq. 1.8.

$$\sqrt{\overline{p_N^2}} = \frac{2}{\pi r_\tau}\sqrt{\beta_\tau^{1/2}\rho_\tau^{1/2}\omega_\tau KT} \qquad (1.8)$$

In this expression r_τ is the sensor tank radius, β_τ is the adiabatic coefficient of cubic elasticity of the fluid filling the sensor tanks, ω_τ is the sensor tank resonant frequency, K is Boltzmann's constant, and T is the absolute temperature.

The input angular rate at which the signal pressure is just equal to the noise pressure above is called the thermal threshold rate or noise equivalent rate and appears as Eq. 1.9.

$$\Omega_N = \left[\frac{(2KT)^{1/2}}{4r_\tau^2 d_d}\right]\left[\frac{1}{p_d}\right]\left[C_\tau^{1/2} C_d \mu_\tau^{1/2}\right] \qquad (1.9)$$

Here d_d is the driver tank width, p_d is the amplitude of the pressure variation in the driver tank, C_τ and C_d are the velocities of sound in the sensor and driver tanks, respectively, and μ_τ is the viscosity of the fluid in the sensor tanks. The remaining symbols are defined beneath Eq. 1.8.

The pressure sensitivity to angular rate input is given by Eq. 1.10

$$S = \frac{p_{\lambda/4}}{\Omega} = \left(\frac{8 d_d}{\pi}\right)\left(p_d\right)\left(\frac{1}{c_d}\right)\left(Q_T\right) \qquad (1.10)$$

where $p_{\lambda/4}$ is the pressure amplitude at the ends of the sensor tank.

D. CONCLUSIONS AND RECOMMENDATIONS

An examination of the form of Eqs. 1.9 and 1.10 discloses the desirability of designing the sensor tanks and choosing a filling fluid to give the highest possible Q and of selecting a filling fluid for the driver tank of low velocity of sound. The addition, it is obviously desirable to operate at reduced temperatures if possible and to drive the fluid in the driver tank as hard as possible.

An example performance calculation using the analysis summarized above for a particular instrument with air chosen as the filling fluid for both the driver and sensor tanks shows that an angular motion sensing instrument of the type described has a thermal threshold rate limit on the order of 10^{-4} earth rates and a pressure sensitivity of a few tenths of a dyne/cm^2 per earth rate. Commercially available pressure transducers have a thermal threshold of their own at pressures of the same order of magnitude as that corresponding to the sensor tank thermal threshold, and thus it is concluded that, although the instrument configuration chosen is not such as to be limited in its performance by its output transducer, present transducers must operate at the limit of their useful sensitivity in this application. The voltage sensitivity of the best of available transducers which were considered in the acoustic rate sensing application for which the calculations were made is slightly below a millvolt per earth rate.

Although liquids offer higher inherent Q's than gases, the present analysis used a gas rather than a liquid in the calculation of the performance figures quoted in the paragraph above. This choice is based on the fact that available transducers of high enough impedance to work into a liquid medium without loading it are not as sensitive as the transducers which are suitable for working into a gas. Moreover, the low compressibility of liquids apparently leads to considerable losses due to wall flexure with an attendent lowering of the actual system Q. Pending further investigation it seems that the use of gases in both the driver and sensor tanks offers the best sensitivity. More study should be given to the problems of wall flexure and tank-transducer impedance matching in an effort to utilize the desirable high Q properties of liquids.

It is felt that a major portion of continued research should be devoted to an investigation of the nature of the coupling mechanism between the driver and sensor tanks. Cross coupling has been advanced as a potential major problem in realizing satisfactory performance with this particular instrument. In the instrument described it is recognized that the assumption of perfect signal quality at the diaphragms and a complete lack of mechanical cross-coupling is unrealistic. An extended noise analysis will certainly be necessary.

In conclusion, the analysis which has been completed indicates that an acoustic angular motion sensor of the type described theoretically is capable of performance competitive with that attainable using conventional rate sensing gyroscopic instruments. A number of areas of the analysis are incomplete, however, and continued investigation will be necessary before firm conclusions as to the feasibility of such an instrument can be drawn.

CHAPTER II

LOSS MECHANISMS AND THE DETERMINATION OF Q

A. THE LOSSLESS CASE

The equations of motion for a fluid element in the simplest case where all dissipative effects are ignored are readily found. Defining the condensation S as the negative divergence of particle position ξ one writes

$$p = p_o + \beta S = p_o - \beta \nabla \cdot \vec{\xi} \tag{2.1}$$

where p is the total pressure, p_o the static pressure, and β the (adiabatic) coefficient of cubic elasticity. Newton's Third Law is next applied to a fluid element to give

$$\rho \ddot{\vec{\xi}} = -\vec{\nabla} p \tag{2.2}$$

where ρ is the static density, $\vec{\nabla} p$ is the gradient of the pressure, and time differentiation is indicated by the conventional dot notation. Equation 2.3 is formed by substituting Eq. 2.1 into Eq. 2.2.

$$\rho \ddot{\vec{\xi}} = \beta \vec{\nabla}^2 \vec{\xi} \tag{2.3}$$

Or

$$\ddot{\vec{\xi}} = \beta/\rho \, \vec{\nabla}^2 \vec{\xi} \tag{2.4}$$

For a plane acoustic wave along the x-axis, Eqs. 2.2 and 2.4 specialize to the scalar equations

$$\rho \frac{\partial \dot{\xi}_x}{\partial t} = - \frac{\partial p}{\partial x} \tag{2.5}$$

and

$$\frac{\partial^2 \dot{\xi}_x}{\partial t^2} = \beta/\rho \frac{\partial^2 \dot{\xi}_x}{\partial x^2} = c^2 \frac{\partial^2 \dot{\xi}_x}{\partial x^2} \tag{2.6}$$

where an additional time differentiation has been performed in Eq. 2.6 since it is desired to retain $\dot{\xi}$ rather than ξ as the fundamental quantity. The velocity of sound is denoted by c. The characteristic acoustic impedance is given by Eq. 2.7.

$$Z_o = \rho c = \sqrt{\beta \rho} \tag{2.7}$$

In the more general case where the system is not lossless, the effects of dissipation can be included in the equations. Losses can be associated with dissipative mechanisms both in the interior of the fluid medium and in the boundary layer where interactions with the walls occur. A number of the more important loss mechanisms will be discussed in the following section and the relative importance of losses in these two regions will be assessed.

B. LOSS MECHANISMS

Three primary mechanisms contribute to losses internal to the medium itself: radiation, heat conduction, and viscous friction. Radiation is associated with the increase and decrease in temperature as the compressions and rarefactions of the wave pass through the medium. There is a net outward radiation of energy as a result of the non-linear character of Stefan's Law. This effect is considered negligible in acoustic wave propagation in fluids.

Of the fluid-wall boundary and the compressions and rarefactions of the medium itself are not wholly adiabatic, heat is conducted through the volume of the fluid and eventually lost to the walls. This effect is comparable in magnitude to the viscous losses considered below.

Viscous losses are present due to internal rates of shearing. Theoretically a plane wave has no shear, but dilatation within the fluid gives rise to effects of this type. Since a fluid has no shear elasticity the shears store no energy, but since a force is necessary to produce the shear work is done which is dissipated as heat.

Theoretical analyses of systems in which only the internal losses discussed above are present yield attainable system Q's of 10^5 and higher.[4] Since the Q's actually measured in acoustic resonators do not approach this figure, being on the order of 10^2 to 10^4, it can be concluded that these internal dissipative mechanisms can be considered negligible in comparison with various losses at the fluid boundaries discussed below.

Since fluid velocity amplitude must drop from some value $\dot{\xi}_o$ on the axis of the tank at the velocity antinode to zero at the walls, there is a great deal of shear, and hence loss, in the boundary layer. The applicable equations are similar in form to those describing electrical skin effect. A model can be chosen in which the bulk of the fluid is contained in a central core within which the velocity amplitude is constant across each cross-section, and the shear is considered to be entirely confined to a boundary layer surrounding this core. This boundary layer is very thin compared with the radius of the tank in high Q resonators. Such a representation is desirable in that the effect of the boundary layer upon the resonant system can be lumped into a single coefficient.

The thickness of the boundary layer can be shown to be proportional to the so-called skin depth δ given in Eq. 2.8.

$$\delta = \sqrt{\frac{2\mu}{\rho\omega}} = \sqrt{\frac{2\nu}{\omega}} \tag{2.8}$$

In this equation μ and ρ are the viscosity and density respectively of the fluid medium, ν is the kinematic viscosity, and ω is the resonant angular frequency. It can, in addition, be shown that a convenient way of representing the effect of the losses introduced by shear in the boundary layer upon the resonator is a complex resistance coefficient $R(\omega)$ formed by considering the losses to be distributed throughout the volume of the tank. The resistance coefficient derived in this manner is given by Eq. 2.9.

$$R(\omega) = \frac{2\mu}{r\delta}(1+j) = \sqrt{\frac{2\mu\rho\omega}{r^2}}(1+j) \tag{2.9}$$

Writing the equations of motion for a lossy medium (with small losses) it is seen that the real part of this resistance coefficient corresponds to a viscous damping and the imaginary part corresponds to an added mass loading. It is demonstrated that in the case where losses are small the boundary layer interactions lower the speed of sound by a second order factor and introduce dispersion. The next section of this chapter calculates the manner in which the Q of the resonant system depends upon the boundary layer losses.

A further loss mechanism which can be classed as a boundary layer interaction results from the elasticity of the tank walls. One might use an approach similar to that by which the boundary layer shear losses were calculated to incorporate into the equations of motion the fact that the walls of the cylinder are not perfectly rigid. Lamb treats wall flexure and calculates the resulting reduction in the speed of sound.[6] The product of his analyses in the special case of walls or infinite thickness is the relation below.

$$c'/c = \sqrt{\frac{K}{K+\beta}} \qquad (2.10)$$

In Eq. 2.10 c' is the new speed of sound, c the old, K the modulus of rigidity of the walls, and β the coefficient of cubic elasticity of the fluid medium. In this special case of infinitely thick walls the effect is negligibly small when gases are used as filling fluids, and the reduction in the speed of sound is not significant with walls of practical thickness. The use of liquids, however, gives β's comparable in size to K, and c' is considerably reduced from c even with infinite wall thickness. For walls of practical thickness the reduction will be some tens of percent and losses in the walls will be intolerable. It may be that wall flexure will be a major obstacle to the use of liquids--with their higher inherent Q's due to lower kinematic viscosities--in the sensing tanks, and it is recommended that further study be directed to this problem.

The amount of power that is extracted from the sensing tanks by the transducers at their ends is a function of the ratio of the transducer impedance to the tank impedance, and thus it will vary both with the choice of filling fluid and the choice of transducer type; i.e., liquid or gaseous fluid, and

capacitive or prezo-electric transducer. The impedance of prezo-electric transducers is much greater than that of capacitive types; in fact, the latter cannot be used with liquid media without loading the sensor tanks considerably. It would seem on the basis of the present investigation that the requirement of small loading by the transducer necessitates the use of a prezo-electric or other solid state transducer if a liquid is chosen as the filling fluid. Inspection of Table A.2 in Appendix A, however, shows that prezo-electric transducers are considerably less sensitive than the capacitive types. It would thus seem that this constitutes another obstacle to the use of liquids as filling media. Further investigation of this problem is recommended.

C. CALCULATION OF Q AND THE PRESSURE AMPLIFICATION FACTOR

An important parameter in the description of any highly resonant system is the so-called quality factor Q. This factor is defined as 2π times the ratio of the total energy stored in the system to the energy dissipated per cycle. Since the boundary layer is very thin in the small loss case, the stored energy is confined almost entirely to the central core of fluid. The time average stored energy in the sensor tank resonant system is just twice the time average kinetic energy, and it can be calculated very simply since the fluid in the core has a constant velocity amplitude at any tank cross-section. A per unit length calculation of Q is adequate although the velocity amplitude is actually sinusoidal with length, for both the stored kinetic energy in the numerator and the rate of dissipation in the denominator are affected equally by this distribution. Eq. 2.11 gives the total energy storage in unit length of the central core at a cross section where the particle velocity amplitude is $\dot{\xi}$.

$$< W > = 2 <T> = 2 < \frac{1}{2} \rho \dot{\xi}^2 \pi r^2 >$$

$$= \frac{1}{2} \rho \dot{\xi}^2 \pi r^2 \qquad (2.11)$$

where $\langle W \rangle$ is the average stored energy and
$\langle T \rangle$ is the average kinetic energy

It can be shown that an expression for the time average power dissipation, $\langle P \rangle$, per unit area of boundary layer bordering on the central core at a point where the particle velocity amplitude is $\dot{\xi}$, is:

$$\langle P \rangle = \frac{\mu \dot{\xi}^2}{2\delta} \tag{2.12}$$

In this expression μ is the fluid viscosity and δ is the skin depth. It is desired to find the power dissipation per unit length of the tank at this cross-section, so it is apparent that $\langle P \rangle$ must be multiplied by the surface of the boundary layer exposed to the central core in unit length, or $2\pi r$. The quantity thus derived will be called $\langle P' \rangle$.

$$\langle P' \rangle = 2\pi r \langle P \rangle = 2\pi r \frac{\mu \dot{\xi}^2}{2\delta} \tag{2.13}$$

From the definition of Q as stated above, it will be seen that Eq. 2.14 gives Q in terms of $\langle W \rangle$ and $\langle P' \rangle$.

$$Q = \frac{\langle W \rangle}{\langle P' \rangle} \omega = r\sqrt{\frac{\rho\omega}{2\mu}} = r/\delta \tag{2.14}$$

The form of this expression is a basis for the statement made earlier that the boundary layer is thin in comparison to the tube radius in highly-tuned resonant systems.

The use of high Q sensor tanks introduces a time constant of $2Q/\omega$ seconds and amplifies the pressure level of the rate signals coupled through the diaphragms. The higher the Q, the closer the position of the diaphragms to true sensor tank pressure modes, for in the low loss case implied by a high Q the power which must be coupled into the sensor tanks to balance boundary layer losses is very small. The pressure amplification factor between the cross-section at the diaphragms and the outer ends of the sensor tanks is calculated by equating this steady state boundary layer loss to the power coupled through the diaphragms by the Coriolis mechanism.

$$\int_{\substack{\text{over area} \\ \text{of} \\ \text{diaphragms}}} p_c \dot{\xi}_o \, dS = \int_0^{\lambda/4} \dot{\xi}^2 R \pi r^2 dx \tag{2.15}$$

The left side of this equation represents the power input at the diaphragms where p_c is the pressure amplitude there and $\dot{\xi}_o$ is the particle velocity amplitude at this velocity antinode. The right side of the equation represents the sensor tank losses. $\dot{\xi}$ varies cosinusoidally from $\dot{\xi}$ at the diaphragms to zero at the outer extremity of the tank, and thus an integration must take place along the x-axis. R is the real part of the resistance coefficient of Eq. 2.9 which was calculated by considering the losses to be distributed throughout the volume of the sensor tank. Inserting this quantity into Eq. 2.15 and performing the integration on the left hand side gives Eq. 2.16.

$$p_c \, \xi_o \pi r^2 = \int_0^{\lambda/4} \dot{\xi}_o^2 \, \frac{2\mu}{r\delta} \, \pi r^2 \cos^2 \frac{2\pi x}{\lambda} \tag{2.16}$$

from which

$$p_c = \frac{2\mu\dot{\xi}_o}{r\delta} \int_0^{\lambda/4} \cos^2 \frac{2\pi x}{\lambda} \, dx \tag{2.17}$$

Substituting $\dot{\xi}_o = -\frac{p_{\lambda/4}}{Z_o} = -\frac{p_{\lambda/4}}{\rho c}$, performing the integration over the length of the tank, and solving for the amplification gives

$$\frac{p\lambda/4}{p_c} = \frac{4r}{\pi\delta} = \frac{4}{\pi} \, Q \tag{2.18}$$

The importance of designing for the highest possible Q is apparent.

CHAPTER III

NOISE, NOISE-EQUIVALENT RATE, AND SENSITIVITY

A. SCOPE OF NOISE ANALYSIS

The assumption is made at the outset that by the employment of double modulation or some more elaborate means all mechanical coupling of driver and sensor tanks has been reduced to negligible proportions. The extent to which this assumption is realistic is impossible to ascertain until further theoretical and experimental work on double modulation techniques has been completed. It is felt, however, that an analysis purely in terms of the fundamental limitation of thermal noise will provide a valuable insight into the ultimate performance of an acoustic angular motion sensor of this type. The analysis below will be restricted to a consideration of thermal noise arising in the sensor tanks. The input pressure signal to these tanks at the diaphragms will be assumed to be of perfect quality.

The primary (non-mechanical) noise in the system will be generated within the sensor tanks. These highly tuned resonators will filter random thermal pressure fluctuations which then will appear as standing waves at the fundamental natural frequency of the tanks. Since this frequency is the one at which output rate signals are sensed, the signal quality at the output transducers will be less than that of the signal coupled in at the diaphragms. A tank output signal to noise figure will be derived assuming perfect signal quality at the diaphragms. This signal to noise ratio will, of course, be proportional to the applied angular rate Ω. By solving for the rate when the signal to noise ratio is unity a thermal noise **equivalent** threshold rate is found. For all rates above this threshold an instrument sensitivity defined as the ratio of output signal pressure to input angular rate will have meaning.

The following analysis while approximate in nature provides relationships which will yield satisfactory maximum performance limits with respect to thermal noise. Of greater limitation is the assumption as to the perfect transmission characteristics of the diaphragm. The two sections following illustrate the steps by which the tank signal to noise ratio, noise equivalent rate, and instrument sensitivity are derived using the simplified noise analysis.

B. THERMAL NOISE PRESSURE AND SENSOR TANK SIGNAL-TO-NOISE RATIO

In the highly tuned system, random pressure fluctuations are filtered by the resonator and appear as standing waves in the tank. The principle of equipartition of energy requires that each quadratic energy storage have assigned to it a mean energy 1/2 KT, where K is **Boltzmann's** constant and T is the absolute temperature. Since time average kinetic and potential energy are equal in a tuned system at resonance, the following expressions hold, the mean being designated by the superscript bar.

$$\overline{\frac{1}{2}\,KT = \frac{1}{2}\,\rho\int\dot{\xi}^2 dV} \;=\; \overline{\frac{1}{2}\beta\int(\nabla\cdot\xi)^2\,dV} \qquad (3.1)$$

Equations 3.2 and 3.3 result from a substitution of $\dot{\xi}$ from Eq. 1.3 into the kinetic energy expression

$$\frac{1}{2}\,KT = \frac{1}{2}\,\rho\int_0^{\lambda/4}\left(\frac{\overline{p_N^2}}{Z_o}\right)\cos^2\frac{2\pi x}{\lambda}\;\pi r^2 dx \qquad (3.2)$$

$$\frac{1}{2}\,KT = \frac{1}{16}\,\rho\,\frac{\overline{p_N^2}}{Z_o^2}\;\pi r^2\lambda \qquad (3.3)$$

The quantity p_N has been introduced as the instantaneous noise pressure. Finally Z_o is eliminated using Eq. 2.7 and the resulting equation is solved for the root mean square noise pressure.

$$\sqrt{\overline{p_N^2}} = \frac{1}{r}\sqrt{\frac{8\beta KT}{\pi\lambda}} = \frac{2}{\pi r}\sqrt{\beta^{1/2}\,\rho^{1/2}\,\omega KT} \qquad (3.4)$$

The sensing tank signal to noise ratio at the output is found on the assumption that the signal pressure p_c coupled in at the diaphragms is noise free. The necessary equations are repeated below for convenience.

$$p_c = 2 d_d \rho d \dot{\xi}_{od} \cos \omega_d t \; \Omega(t) \tag{1.5}$$

$$p_{\lambda/4} = \frac{4r_T}{\pi \delta_T} p_c \tag{1.7}$$

$$\delta_T = \sqrt{\frac{2\mu_T}{\rho_T \omega_T}} \tag{2.8}$$

The signal to noise ratio is written directly by the use of these expressions.

$$(S/N)_T = \frac{p\lambda/4}{\sqrt{\rho_N^2}} = \left[\frac{4r_T^2 \, d_d}{(2KT)^{1/2}}\right]\left[p_d \Omega(t)\right]\left[\frac{\rho_T^{1/4} \, \rho_d^{1/2}}{\beta_T^{1/4} \beta_d^{1/2} \mu_T^{1/2}}\right] \tag{3.5}$$

Substituting $c = \beta/\rho$ in this expression gives a slight simplification

$$(S/N)_T = \left[\frac{4r_T^2 \, d_d}{(2KT)^{1/2}}\right]\left[p_d \Omega(t)\right]\left[\frac{1}{c_T^{1/2} \, c_d \, \mu_T^{1/2}}\right] \tag{3.6}$$

This equation is grouped in three factors. The first of these contains the apparatus dimensions and the ambient temperature, the second contains the driver pressure amplitude, and the third contains the parameters fixed by the choice of filling fluids in the driver and sensor tanks.

C. THRESHOLD RATE AND SENSITIVITY

The input angular rate at which $(S/N)_T$ is unity is called the thermal threshold rate or the thermal noise equivalent rate and is found from Eq. 3.6.

$$\Omega_N = \left[\frac{(2KT)^{1/2}}{4r_T^2 \, d_d}\right]\left[\frac{1}{p_d}\right]\left[\frac{\beta_T^{1/4} \, \beta_d^{1/2} \, \mu_T^{1/2}}{\rho_T^{1/4} \, \rho_d^{1/2}}\right]$$

$$= \left[\frac{(2KT)^{1/2}}{4r_T^2 \, d_d}\right]\left[\frac{1}{p_d}\right]\left[c_T^{1/2} \, c_d \, \mu_T^{1/2}\right] \tag{3.7}$$

For input rates above this thermal threshold a meaningful instrument sensitivity can be defined; this sensitivity is simply the output signal pressure amplitude per unit input angular rate.

$$S = \frac{P_{\lambda/4}}{\Omega} = \left[\frac{4\sqrt{2}\, r_T d_d}{\pi}\right]\left[p_d\right]\left[\omega_T^{1/2}\right]\left[\frac{\rho_T^{1/2}\ \rho_d^{1/2}}{\mu_T^{1/2}\beta_d^{1/2}}\right] \qquad (3.8)$$

Note that a fourth factor appears in this expression, indicating that the sensitivity is a function of frequency. This fact allows the incorporation of Q into the sensitivity expression to give Eq. 3.9

$$S = \left[\frac{8d_d}{\pi}\right]\left[p_d\right]\left[\frac{1}{c_d}\right]\left[Q_T\right] \qquad (3.9)$$

It is seen that the instrument sensitivity is directly proportional to the Q of the sensor tanks, to the pressure amplitude in the driver tank, and to the distance between the diaphragms. In addition, it is desirable both from Eq. 3.7 and Eq. 3.9 to choose a fluid in the driver tank whose speed of sound is as low as possible. These requirements alone would indicate that a gas should be used in the driver tank and a liquid in the sensor tanks. The difficulty discussed above of finding transducers capable of working with sufficient sensitivity into a liquid medium, together with the introduction of wall flexure problems attendant upon the use of a liquid, raises questions as to whether the use of liquids is indeed indicated. Until such time as continued investigation resolves these questions, it is deemed prudent to illustrate the performance analyses using a fluid in the gaseous state in both the driver and sensor tanks. Such a sample calculation is carried out in Appendix A for a particular choice of instrument dimensions and filling gas.

APPENDIX A

EXAMPLE PERFORMANCE CALCULATION

Air at atmospheric pressure and 300°K is selected as the filling fluid for both the driving and sensing tanks. The acoustic properties of air under these conditions are presented in Table A.1. The pressure amplitude in the driving tank is chosen to be 10^5 dynes/cm^2 or one tenth atmosphere pressure. This choice gives a velocity amplitude at the velocity antinode of roughly 8 % of the velocity of sound. This is felt to be a conservative level, and it will be recognized that an improvement in threshold rate and sensitivity of up to a factor of ten may be achieved if it is found possible to drive the air at velocities closer to C.

Table A.2 presents the sensitivities of pressure transducers suitable for use in an acoustic angular motion sensing application. The Western Electric 640AA condenser microphone is selected as the pressure transducer since it is the most sensitive available. The noise generated within this microphone when it is working across a 50 MΩ resistor into a tuned pre-amplifier of 10 cycle bandwidth is such that its signal to noise figure is unity at an input pressure of 6×10^{-5} dynes/cm^2. Ω_N will be given below as the lowest rate at which both (S/N) 640AA and $(S/N)_\tau$ exceed unity. This threshold will be very slightly larger than that given by the first condition alone, illustrating that instrument sensitivity is not limited by the transducer, but rather by thermal noise in the sensing tanks.

Table A.3 below summarizes the results of the performance calculation for the air-air system using the particular instrument dimensions tabulated therein. Note that the sensing tank length chosen fixes the tank frequency at 2100 cps. The frequency in the driver is separated from this by the mechanical spin frequency which will necessarily be considerably smaller; hence $f_d \doteq f_\tau$, and since the choice of the same gas for driving and sensing tanks gives $c_d = c_\tau$ and $\lambda_d = \lambda_\tau$.

The Q of 206 is generally representative of what will be obtained using any gas in tanks of this size. The use of liquids permits the attainment of Q's perhaps an order of magnitude above this subject to the difficulties enumerated in the body of this report.

Table A.1

Acoustic Properties of Air at
Atmospheric Pressure and 300°K

ρ	in	g/cm^3	1.2×10^{-3}
μ	in	poise	1.83×10^{-4}
ν	in	cm^2/sec	1.5×10^{-1}
c	in	cm/sec	3.32×10^{4}
z_o	in	$\frac{dyne\ sec}{cm^3}$	4.0×10^{1}

Table A.2

Transducer Sensitivities

Manufacturer and Type	Sensitivity in db re 1 volt re 1 μbar	Max db for linearity re .0002 μbar	Freq. resp. between 3 db pts in cps.
Altec-Lansing[7] 21BR180-5 (condenser)	-70	170	10-8000
Atlantic Research[7] BD-10 ($Ba\ Ti_3$)	-111	230	1-2000
Endevco Corp.[7] 2501 (Prelectric)	-125	224	2-10000
Western Electric[8] 640AA (condenser)	-50	134	10-12000

Table A.3

Summarized Results of Performance Analysis of the Air-Air System

	$r_T = 1$ cm $\quad d_d = 2$ cm
$T = 300^{\circ}K$	$l_d = 2l_T = 8$ cm
$\rho_o = 10^6$ dynes/cm^2	$f_T \doteq f_d = 2100$ cycles/sec
$\rho_d = 10^5$ dynes/cm^2	$\delta = 4.9 \times 10^{-3}$ cm = 1.9 mils
$Q_T = 206$	$\dot{\xi}_{od} = 2.5 \times 10^3$ cm/sec
$\Omega_N = 2.9 \times 10^{-8}$ rad/sec $= 4.2 \times 10^{-4}$ ER*	
$S = 2.3 \times 10^{-1}$ dynes/cm^2/ER $= 6.9 \times 10^{-4}$ volts/ER	

* Tank noise limited: multiply by 0.65 for transducer limit.

BIBLIOGRAPHY

1. Granquist, Care-Erik; "Gyroscope Device with Vibratory Gas Particles or Particles of Another Sound Transferring Medium," U.S. Patent No. 2,999,389; Patented September 12, 1961.

2. Morrow, C.T., "Zero Signals in Sperry Tuning Fork Gyrotron," J. Acoustical Society of America, 27, 581-85 (1955).

3. Germain, Lloyd and Thomas Wing, "Crystal Rate Gyro" Gulton Industries Inc., Metuchen, N.J. ASD Technical Report 61-253 on Air Force Contract No. AF33(616)-5561, August 1961.

4. Heuter, T.F. and Bolt, R. H., Sonics, John Wiley and Sons, Inc., N.Y., (1955), p. 25.

5. Crandall, Vibrating Systems and Sound, D. Van Nostrand Co., Inc., N.Y. 1927.

6. Lamb, Memoirs of the Manchester Literary and Philosophical Society, 42, (1898).

7. Kamperman, Noise Control, "Measurement of High Intensity Noise," September 1958, p. 22.

8. Hawley, M.S., "The Condenser Microphone as an Acoustic Standard," Bell Laboratories Record, 33, 6-10, (1955).